



# Absorption and photoluminescence studies of $\text{CdGa}_2\text{S}_4:\text{Cr}$

M.B. Johnson <sup>a,\*</sup>, S.B. Mirov <sup>a</sup>, V. Fedorov <sup>a</sup>, M.E. Zvanut <sup>a</sup>,  
J.G. Harrison <sup>a</sup>, V.V. Badikov <sup>b</sup>, G.S. Shevirdayeva <sup>b</sup>

<sup>a</sup> Department of Physics, The University of Alabama at Birmingham, 1300 University Boulevard,  
UAB Birmingham, AL 35294-1170, USA

<sup>b</sup> Kuban State University, Krasnodar 350640, Russia

Received 26 October 2003; received in revised form 11 January 2004; accepted 23 January 2004

## Abstract

The potential of using ternary defect chalcopyrites as laser active materials is investigated by performing absorption, photoluminescence, and EPR studies of as-grown and vacuum annealed Cr-doped  $\text{CdGa}_2\text{S}_4$ . Although no consistent affect of annealing is observed, an increased concentration of Cr in the melt during growth is shown to broaden an absorption band at 1288 nm. Several of the absorption bands could be attributed to multiple charge states of Cr thought to be present in the crystal. A broad fluorescence was observed at visible wavelengths; however, no emission was detected in the middle-infrared region, contrary to expectation. The lack of infrared fluorescence may be attributed to an exchange interaction involving Cr impurities.

© 2004 Elsevier B.V. All rights reserved.

PACS: 33.20.Ea; 33.50-j

Keywords: Defect chalcopyrite;  $\text{CdGa}_2\text{S}_4$ ;  $\text{CdGa}_2\text{S}_4:\text{Cr}$ ; Absorption; Optical studies; Photoluminescence

## 1. Introduction

Divalent transition metals, particularly chromium, can be used in II–VI materials such as ZnSe and ZnS to produce broadly tunable continuous wave middle-infrared (mid-IR) lasers [1]. Recent investigations demonstrate that ternary com-

pounds may also be used to create middle infrared lasers. For example, Nostrand and coworkers show that the  $\text{Dy}^{3+}$  doped ternary compound  $\text{CaGa}_2\text{S}_4$ , an orthorhombic ternary compound with a space group of  $D_{2h}^{24}$ , lases from 4300 to 4400 nm at room temperature with a pump wavelength of 1319 nm [2]. Our work focuses on the potential of the  $\text{CdGa}_2\text{S}_4$  doped with Cr as a laser-active material.  $\text{CdGa}_2\text{S}_4$  has a space group of  $S_4^2$  and is classified as a defect chalcopyrite, a material that is differentiated from the chalcopyrite structure by stoichiometric vacancies within the crystal lattice. Chalcopyrites and defect chalcopyrites are tetra-

\* Corresponding author. Tel.: +1-2563039351; fax: +1-2059348042.

E-mail address: [mbj@uab.edu](mailto:mbj@uab.edu) (M.B. Johnson).

hedrally bonded like the II–VI compounds, but the crystal field splitting is smaller than in the binary materials. The smaller crystal field splitting implies that doped ternary chalcopyrites should be expected to emit radiation at longer wavelengths than the II–VI crystals.

The band gap of  $\text{CdGa}_2\text{S}_4$  has a range of reported values in the scientific literature varying from 3.77 eV [3] to 3.07 eV [4]. The undoped material is transparent from 400 to 13,000 nm [4], and, when excited at 80 K by light with wavelength 365 and 313 nm, shows a broad fluorescence band from 451 to 425 nm [3]. Thermally stimulated luminescence (TSL) and thermally stimulated conductivity (TSC) measurements indicate that the concentration of intrinsic defects in  $\text{CdGa}_2\text{S}_4$  is 2.5 mol%. These defects exist primarily as compensated donor–acceptor pairs [5]. Studies of dopants in  $\text{CdGa}_2\text{S}_4$  include photoluminescence (PL) of Cd [3] absorption of Co [6], electron paramagnetic resonance (EPR) of Cr [7], as well as a variety of experiments that address the effects of Ag and In [5]. The goal of our research is to investigate absorption, PL, and EPR of Cr-doped  $\text{CdGa}_2\text{S}_4$  to determine the potential for this material to lase in the mid-IR.

## 2. Experimental

The samples of  $\text{CdGa}_2\text{S}_4$  and  $\text{CdGa}_2\text{S}_4$  doped with chromium in the melt ( $\text{CdGa}_2\text{S}_4:\text{Cr}$ ) were grown by the Bridgeman–Stockbarger method. All samples had one face optically polished and were varying shades of pale yellow and topaz. The concentration of chromium in the melt during growth of the topaz crystals was greater than that used during growth of the pale yellow crystals; thus, it is likely that there is a higher density of Cr in the topaz than in the pale yellow samples. One doped crystal of each color was annealed for 12 h in vacuum at 900 K. X-ray diffraction measurements showed that all samples are single crystal with the full width at half maximum (FWHM) of the diffraction peaks ranging from  $0.01^\circ$  to  $0.1^\circ$ , values similar to those reported by others [8].

A Shimadzu spectrophotometer was used for optical absorption analysis up to 2900 nm, and a

Melles Griot linear polarizer, model number 03-FPI-005, was used to analyze the polarization dependence of absorption in the 500–2500 nm range. PL measurements and absorption measurements from 2900 to 5000 nm were performed with a nitrogen purged 0.75 and 0.3m Acton Research “SpectraPro” spectrometers and a TE cooled PbS or liquid nitrogen cooled InSb fast (0.7  $\mu\text{s}$ ) detector. An Oriel tungsten-halogen lamp was used for absorption measurements above 2900 nm. The absorption curves were analyzed with PeakFit Version 4 software.

The excitation at 354 nm for PL measurements was provided by a SpectraPhysics GCR230 Nd:YAG laser. A frequency doubled  $\text{LiF:F}_2^{+**}$  color center laser was used to provide the excitation at 450 nm. A 300 mW erbium fiber laser, model ED-2 from IPG Photonics Corporation, produced the 1560 nm light used in PL measurements. PL measurements with 2500 nm excitation used a homemade erbium fiber laser pumped  $\text{Cr}^{2+}:\text{ZnS}$  laser. For PL measurements at 77 K using 1560 nm excitation the radiation was directed to the sample placed in a homemade cryostat through a quartz rod that absorbs all radiation from 2500 to 2700 nm and 3300 to 4000 nm.

A Bruker 200 X-band (9.6 GHz) spectrometer was used to conduct the EPR experiments. This system is equipped with a Varian model 3609 electromagnet, which provided magnetic fields from 500 to 7500 G. Low temperature EPR experiments utilized either an Air Products closed cycle helium refrigerator connected to a Lakeshore temperature controller, or an Oxford Instruments ESR 900 cryostat unit. All EPR spectra were taken of samples that had been in a dark cavity for a minimum of 12 h.

## 3. Results and discussion

Absorption measurements confirmed that the undoped  $\text{CdGa}_2\text{S}_4$  samples are transparent in the range from 450 to 3000 nm [4]. The unpolarized absorption spectra of the unannealed topaz and pale yellow  $\text{CdGa}_2\text{S}_4:\text{Cr}$  crystals are shown in Fig. 1 curves a and b, respectively. The absorption

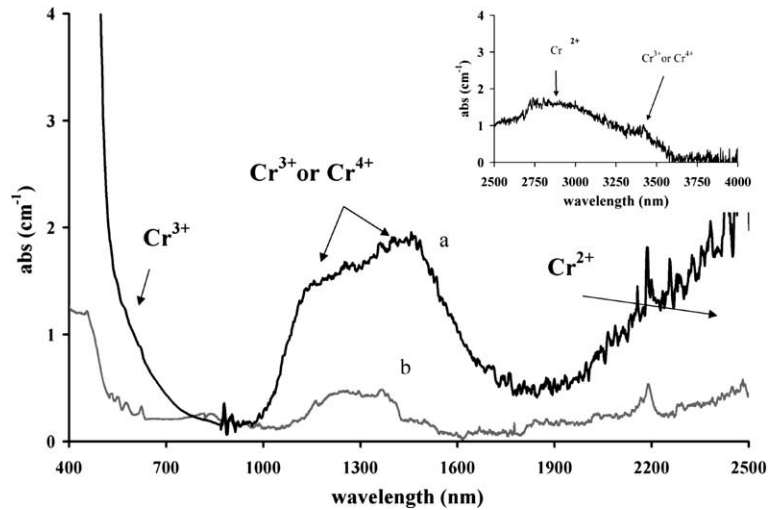


Fig. 1. Room temperature unpolarized absorption of band centered at 1288 nm in pale yellow annealed (●) and unannealed (△)  $\text{CdGa}_2\text{S}_4:\text{Cr}$ . Optical excitation was incident on the (114) plane.

bands of the annealed  $\text{CdGa}_2\text{S}_4:\text{Cr}$  crystals are the same as those in the unannealed samples. Accurate fitting of the absorption spectra required as many as 10 Gaussian shaped curves, ranging from 450 to 3400 nm. Here, we focus primarily on a band centered at 1288 nm. Fig. 1 indicates that in the topaz crystal this absorption band is about 300 nm broader than that seen in the pale yellow crystals. The direction of the dipole moment associate with the absorption band at 1288 nm was determined to be [001] by polarized absorption measurements with the light incident on the (110) plane and polarized with reference to [001], which is the optical axis for the undoped  $\text{CdGa}_2\text{S}_4$  crystals. The absorption band at 1288 nm in the topaz crystals cannot be fit to a Gaussian shape at any polarization angle. However, the absorption spectra of the pale yellow crystals yield Gaussian lineshape centered at 1288 nm at all angles of linear polarization measured. It is likely that the broader linewidth and polarization-dependent lineshape result from the larger Cr concentration thought to be present in the topaz crystals as compared the pale yellow samples. High impurity concentrations are known to produce inhomogeneous broadening and/or additional absorption bands from pairing between the dopant atoms or additional intrinsic defects.

As mentioned above, the absorption band at 1288 nm was found to be polarization dependent in both the pale yellow and topaz samples. Fig. 2 illustrates the results obtained from the unannealed (△) and annealed (●) pale yellow  $\text{CdGa}_2\text{S}_4:\text{Cr}$  crystals, and Fig. 3 shows data obtained from the topaz crystals. Since both the pale yellow and topaz crystals display very similar polarization dependence of absorption bands, we investigated the variations of polarization dependence with incident face by orienting the two sets of crystals differently. The pale yellow crystals are oriented such that light is incident on the (114) face, and the topaz crystals are oriented such that light is incident on the  $(\bar{1}01)$  face. In both sets of crystals the polarization angle is measured in degrees from the [112]. The coefficient of absorption of the heavily doped topaz crystals was greater than scale of Fig. 3 for polarization angles between  $135^\circ$  and  $150^\circ$ . The heavily doped annealed crystal show a reduction in absorption at the 1288 nm band when compared to the unannealed crystal. This is change of absorption with annealing of the topaz crystals is in contrast to the pale yellow crystals, which show little change in absorption at 1288 nm with annealing. Low temperature measurements more clearly resolve a few of the absorption bands extracted from the unpolarized measurement

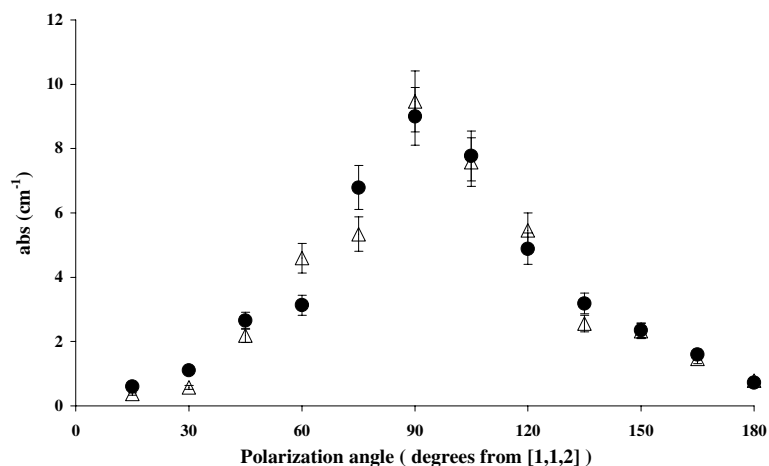


Fig. 2. Room temperature polarized absorption of band centered at 1288 nm in pale yellow annealed (●) and unannealed (Δ) CdGa<sub>2</sub>S<sub>4</sub>:Cr. Optical excitation was incident on the (1, 1,  $\bar{4}$ ) plane.

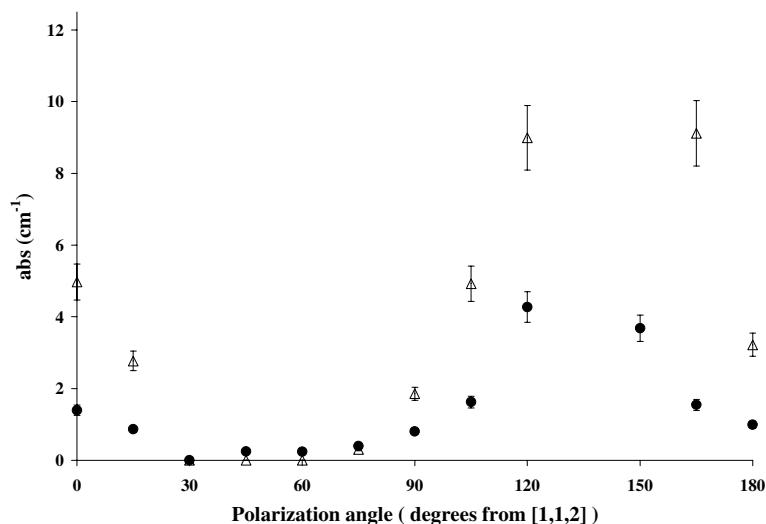


Fig. 3. Room temperature polarized absorption of band from 1100 to 1400 nm measured in topaz CdGa<sub>2</sub>S<sub>4</sub>:Cr. Optical excitation was incident on the ( $\bar{1}01$ ) plane for the unannealed sample (Δ), and annealed sample (●).

shown in Fig. 1. Fig. 4 shows the results obtained for the annealed topaz CdGa<sub>2</sub>S<sub>4</sub>:Cr crystal obtained at 300 K (a) and 13 K (b). The temperature dependence of the band at 1430 nm suggests that the absorption is a phonon assisted transition. When this band vanishes at low temperature, the 1530 nm band is clearly resolved.

Although it is difficult to interpret the source of all of the absorption bands observed in these

crystals, basic crystal field theory calculations indicate that several bands seen in the CdGa<sub>2</sub>S<sub>4</sub>:Cr crystals may be due to chromium in a tetrahedral environment. To justify attributing the optical results to Cr, we note that no infrared absorption was observed in the undoped samples. Furthermore, there were no defects detected by our 9.6 GHz EPR measurements of the undoped crystals. EPR experiments performed by others at 65–240

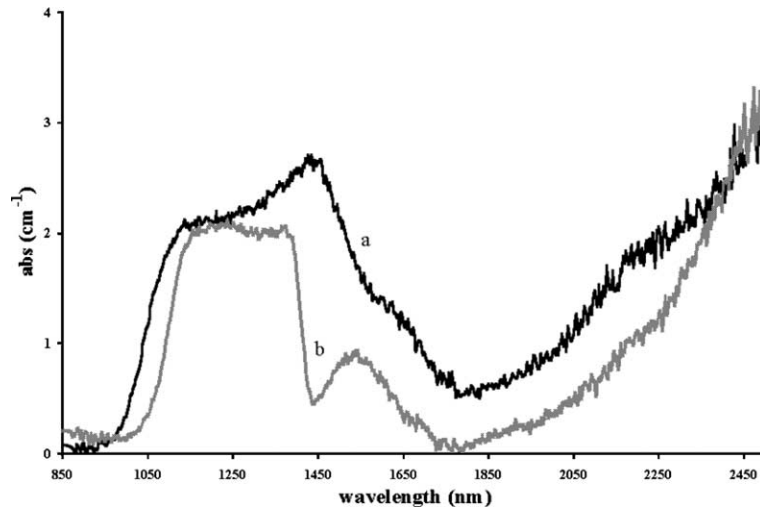


Fig. 4. Temperature dependence of the unpolarized absorption spectra for annealed topaz  $\text{CdGa}_2\text{S}_4:\text{Cr}$  crystal. The spectra were measured at (a) 300 K and at (b) 13 K.

GHz on similar  $\text{CdGa}_2\text{S}_4:\text{Cr}$  crystals indicate the  $\text{Cr}^{2+}$  ion exists in a tetrahedral environment [7]. To predict the absorption due to chromium in  $\text{CdGa}_2\text{S}_4$  a simple analysis was done utilizing Tanabe–Sugano diagrams and the Racah  $B$  parameter for the free ions. The crystal field splitting of  $3640\text{ cm}^{-1}$  for  $\text{CdGa}_2\text{S}_4$  was determined from absorption data of  $\text{Co}^{2+}$  in  $\text{CdGa}_2\text{Se}_4$  and  $\text{CdGa}_2\text{S}_4$  [6,9]. Because this crystal field splitting is small, the free ion Racah  $B$  parameter can be used as an approximation, and Hund's rule is expected to apply. For  $\text{Cr}^+$ ,  $\text{Cr}^{2+}$ ,  $\text{Cr}^{3+}$ , and  $\text{Cr}^{4+}$  calculations were performed with the free ion Racah  $B$  parameters of 710, 830, 1030 and  $1039\text{ cm}^{-1}$ , respectively [10]. This analysis found that no optical absorption is to be expected for  $\text{Cr}^+$  in  $\text{CdGa}_2\text{S}_4$ , which does not preclude  $\text{Cr}^+$  from existing within the crystal. Listed in Table 1 and shown in Fig. 1 are the wavelengths of predicted absorption bands

for the different valence states of chromium and the experimentally determined absorption bands that may be associated with each transition within chromium. The remaining absorption bands, which could not be linked to transitions within the chromium atom assuming a tetrahedral symmetry, may reflect the presence of intrinsic defects created by the incorporation of Cr into the lattice.

Photoluminescence was performed at room temperature and 77 K using excitation wavelengths at the absorption bands attributed to chromium, and with band-to-band excitation of 355 nm. Low temperature PL was performed for excitation wavelengths of 355, 450, 1500 and 2500 nm. No fluorescence was detected from the sample at room or low temperature when excitation of 450, 1500, or 2500 nm was utilized. It should be noted that the low temperature PL measurements at 77 K with excitation at 2500 nm utilized a

Table 1

Absorption bands in  $\text{CdGa}_2\text{S}_4:\text{Cr}$  attributed to the different charge states of Cr in a tetrahedral environment

Transition	$\text{Cr}^{2+}$	$\text{Cr}^{3+}$			$\text{Cr}^{4+}$	
	${}^5\text{T}_2 - {}^5\text{E}$ (nm)	${}^4\text{T}_1({}^4\text{F}) - {}^4\text{T}_1({}^4\text{P})$ (nm)	${}^4\text{T}_1 - {}^4\text{T}_2$ (nm)	${}^4\text{T}_1 - {}^4\text{T}_2$ (nm)	${}^3\text{T}_{2g} - {}^3\text{T}_g$ (nm)	${}^3\text{T}_{2g} - {}^3\text{T}_{2g}$ (nm)
Experimental	2855	520	1288	3400	1288	3400
Calculated	2700	500	1400	3250	1370	3200

quartz rod to direct radiation to the detector. The quartz rod has transmission windows below 2525 nm and between 2700 and 3300 nm. Hence, it is possible that the quartz rod absorbed fluorescence of the 2500 nm excitation at 77 K. The only measurable fluorescence in the pale yellow crystal occurred when using band to band excitation of 355 nm at 77 K. This fluorescence is very weak and similar to that observed by others studying undoped  $\text{CdGa}_2\text{S}_4$ ,  $\text{CdGa}_2\text{S}_4\text{:In}$ , and of  $\text{CdGa}_2\text{S}_4\text{:Ag}$  [11]. The fluorescence in the undoped  $\text{CdGa}_2\text{S}_4$ ,  $\text{CdGa}_2\text{S}_4\text{:In}$ , and of  $\text{CdGa}_2\text{S}_4\text{:Ag}$  crystals was attributed to donor–acceptor pair recombination.

Crystal field theory predicts that chromium should fluoresce at mid-IR wavelengths; therefore, the lack of PL emission in the Cr-doped samples suggests that the crystal contains additional defects that interact with the chromium impurities and quench the fluorescence. Evidence of these defects appears in X-band (9.6 GHz) EPR measurements of the samples which showed two broad resonance lines with strongly angular dependent line position, linewidth, and lineshape. The resonance values, linewidth, and lineshape did not vary from 12 to 200 K. Below, the EPR data are presented and the possible relationship between the defects and quenched luminescence is discussed.

The undoped  $\text{CdGa}_2\text{S}_4$  crystal did not produce any EPR spectra; however, both the annealed and

unannealed doped crystals showed two resonance lines. Fig. 5 illustrates the angular dependence of the X-band EPR resonances observed in  $\text{CdGa}_2\text{S}_4\text{:Cr}$  crystals that were rotated about the (001) axis ( $\square$ ), (112) axis (x), the (227) axis ( $\blacktriangle$ ), and the (314) axis ( $\bullet$ ). The initial angle has been adjusted to account for the uncertainty of orienting the sample in the cavity and to emphasize the similarity of the data in all rotation planes. EPR data plotted in the manner of Fig. 5 typically provide the symmetry of the defect by fitting Eq. (1) to the experimental data [12].

$$g^2 = g_1^2 \cos(\theta_1) + g_2^2 \cos(\theta_2) + g_3^2 \cos(\theta_3). \quad (1)$$

Here,  $g$  is the electronic  $g$  factor obtained from the magnetic field at which a resonance occurs. The  $g_1$ ,  $g_2$ , and  $g_3$  are the principle values of the electronic  $g$  tensor and  $\theta_1$ ,  $\theta_2$ , and  $\theta_3$  are the angles between the principle axes and the applied magnetic field [12]. When a crystal is rotated about different axes, the  $g$  value should vary as the angles between principle axes and the applied magnetic field,  $\theta_1$ ,  $\theta_2$ , and  $\theta_3$ , change. By examining Fig. 5 it can be seen that the data of  $\text{CdGa}_2\text{S}_4\text{:Cr}$  does not vary significantly between rotation planes. For this reason, the typical analysis used to determine defect symmetry may not be performed. To distinguish the two centers the two resonance lines are referred to as the  $g = 6$  and the  $g = 3$  resonance,

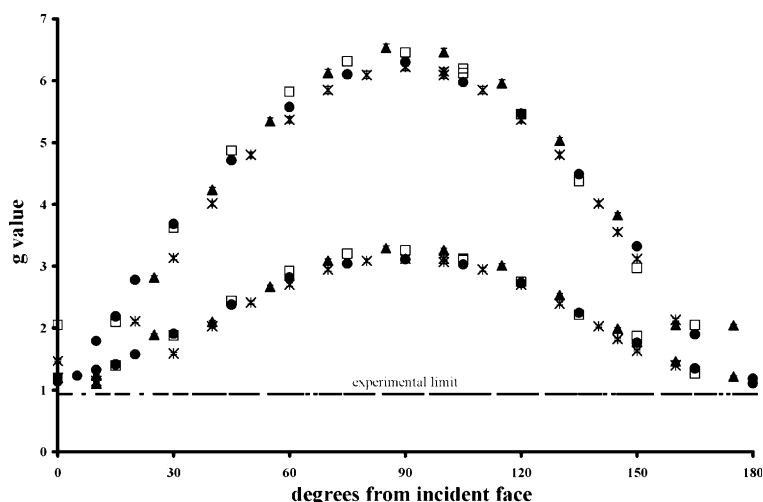


Fig. 5. Angular variation of X-band EPR resonance lines being studied for rotation about the [001] ( $\square$ ), the [112] (x), the [114] ( $\blacktriangle$ ), and the [314] ( $\bullet$ ).

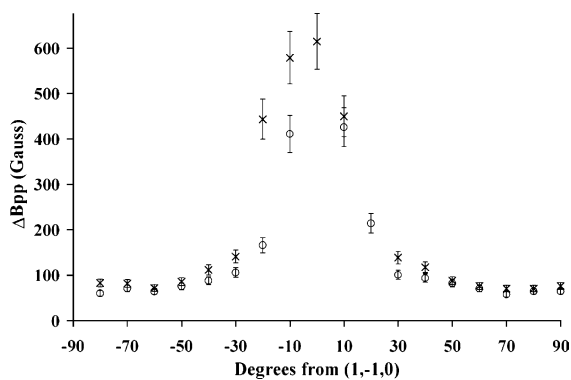


Fig. 6. The variation of the peak-to-peak linewidth,  $\Delta B_{pp}$ , of the first derivative signal of X-band EPR resonance with angle for rotation about the [1,1,2] for the  $g = 6$  resonance (○) and the  $g = 3$  resonance (x).

which denote the maximum  $g$  value associated with each resonance line.

As illustrated in Fig. 6, the peak-to-peak linewidth,  $\Delta B_{pp}$ , of the  $g = 6$  (x) and  $g = 3$  (o) signals in the  $\text{CdGa}_2\text{S}_4:\text{Cr}$  crystals display an angular variation from 58 to 615 G. The angular dependence of the lineshape of the resonances from  $\text{CdGa}_2\text{S}_4:\text{Cr}$  crystals was analyzed and found to be Lorentzian near the center of the resonance for the most narrow linewidths. The X-band EPR resonances became increasingly Gaussian as the linewidth increased, and could be fit with a pure Gaussian curve at the widest peaks.

The angular variation of the linewidth, lineshape, and line position among several rotation planes is consistent with exchange narrowing [13,14]. For example, exchange narrowed EPR signals should have large angular variations in linewidth as shown in Fig. 6 [13]. Also, exchange narrowed resonance lines are required to have a Lorentzian lineshape near the center of the resonance and may become purely Gaussian when the sample is rotated through the direction of dipole–dipole interaction, as is observed in our data [15]. Finally, the similarity of the angular dependence of the resonance line position in all rotation planes (Fig. 5) is consistent with the presence of exchange interactions, which reduce the  $g$  values of each center to the average value appropriate for each rotation plane [14].

The structural or chemical identity of the defects may not be extracted directly from our X-band EPR data; however, Avanesov and coworkers performed 65–240 GHz EPR studies on  $\text{CdGaS}:\text{Cr}$  grown in a manner similar to our samples [7]. At these high frequencies the microwave energy is large enough to probe the Cr d-shell spin transitions. As a result, the data could be analyzed with the appropriate EPR theory and the spectrum was assigned to  $\text{Cr}^{2+}$ . Their detection of Cr in crystals similar to those used in our studies, coupled with the lack of EPR signals in our undoped samples and the assignment of some of the absorption bands to Cr transitions suggests that various charge states of chromium may be responsible for one or both of the signals observed at 9.6 GHz. If this assignment is correct and if the EPR data are interpreted in terms of exchange narrowing, the absence of the infrared luminescence expected from chromium may be attributed to interaction of Cr with additional defects by means exchange coupling. The literature of  $\text{CdGa}_2\text{S}_4$  indicates that defect densities in the undoped material may be as high as 2.5 mol% [5], making the concept of closely spaced centers capable of electron exchange feasible. Exchange interactions may provide a mechanism for energy transfer from chromium to other defects, which relax without emitting radiation [16]. The unidentified absorption lines may be another consequence of the exchange coupling within the system of ions [17]. Clearly, further EPR studies are necessary to clarify the role of Cr, and possibly exchange, in the quenching of the luminescence.

#### 4. Summary

Two sets of Cr-doped  $\text{CdGa}_2\text{S}_4$  crystals were studied before and after vacuum annealing at 900 °C. Both sets of Cr-doped  $\text{CdGa}_2\text{S}_4$  crystals exhibited an absorption spectrum between 450 and 3500 nm that could be resolved into 10 absorption bands, and both sets of Cr-doped  $\text{CdGa}_2\text{S}_4$  crystals revealed a polarization dependent absorption intensity for a band centered at 1288 nm. However, the topaz colored crystals exhibited evidence of a higher density of intrinsic defects than the pale yellow crystal. We attribute the higher density of

intrinsic defects in the topaz colored crystals to the larger concentration of Cr present in the melt during growth of the topaz colored samples. Based on crystal field calculations, absorption bands seen in the Cr-doped CdGa<sub>2</sub>S<sub>4</sub> crystals at 520 nm could be attributed to Cr<sup>3+</sup>, and one at 2855 to Cr<sup>2+</sup>. The predicted absorption bands for Cr<sup>3+</sup> and Cr<sup>4+</sup> in CdGa<sub>2</sub>S<sub>4</sub> fit equally well the two other absorption bands at 1288 and 3400 nm. At 77 K fluorescence of Cr-doped CdGa<sub>2</sub>S<sub>4</sub> with band to band excitation of 355 nm light was observed in the visible region, which is similar to results from band to band PL of CdGa<sub>2</sub>S<sub>4</sub> doped with In or Ag. Further work will be done to determine whether the lack of expected fluorescence in the mid-IR may be attributed to an exchange interaction involving the Cr impurities.

## References

- [1] L. Deloach, R. Page, G. Wilke, S. Payne, W. Krupke, IEEE J. Quant. Electron. 32 (1996) 885.
- [2] M.C. Nostrand, R.H. Page, S.A. Payne, W.F. Krupke, P.G. Schunemann, Opt. Lett. 24 (1999) 1215.
- [3] A.N. Georgobaini, V.S. Donu, Z.P. Illyukhine, V.I. Pavelnko, I.M. Tiginyanu, Sov. Phys. Semicond. 17 (1983) 970.
- [4] K.R. Allakhverdiev, Z.Yu. Salaeva, A.B. Orun, Opt. Comm. 167 (1999) 95.
- [5] P. Kivits, M. Wijnakker, J. Claassen, J. Geerts, J. Phys. C 11 (1978) 2361.
- [6] C. Kim, T. Cho, J. Kim, W. Kim, H. Park, Phys. Rev. B. 36 (1987) 9283.
- [7] A.G. Abonesov, V.V. Badikov, G.S. Shakurov, Phys. Sol. State 45 (2003) 1451.
- [8] G. Kimmel, Y. Shimony, O. Raz, M.P. Dariel, Mater. Struct. 6 (1999) 149.
- [9] Y. Kim, C. Kim, W. Kim, J. Kor. Phys. Soc. 40 (2002) 952.
- [10] B. Di Bartolo, Optical Interactions in Solids, John Wiley and Sons, New York, 1968.
- [11] P. Kivits, Thermoluminescence and Thermally Stimulated Conductivity in CdGa<sub>2</sub>S<sub>4</sub> Including Evaluation and Some Extensions of the Conventional Two Level Model, University of Eindhoven, Eindhoven, 1976.
- [12] J. Weil, J. Bolton, J. Wertz, Electron Paramagnetic Resonance Elementary Theory and Practical Applications, John Wiley & Sons, New York, 1994.
- [13] A. Bencini, D. Gatteschi, EPR of Exchange Coupled Systems, Springer-Verlag, New York, 1990.
- [14] F.E. Mabbs, D. Collison, Electron Paramagnetic Resonance of d Transition Metal Compounds, Elsevier, New York, 1992.
- [15] P.W. Anderson, P.R. Weiss, Rev. Mod. Phys. 25 (1953) 269.
- [16] C.Z. Hadad, S.O. Vasquez, Phys. Rev. B 60 (1999) 8586.
- [17] J. Furgeson, H.J. Guggenheim, Y. Tanabe, Phys. Rev. Lett. 14 (1965) 737.